Matching-pursuit split-operator Fourier-transform simulations of excited-state intramolecular proton transfer in 2-(2′-hydroxyphenyl)-oxazole

Yinghua Wu[a] and Victor S. Batista[b]
Department of Chemistry, Yale University, P.O. Box 208107, New Haven, Connecticut 06520-8107

(Received 6 March 2006; accepted 14 April 2006; published online 9 June 2006)

The excited-state intramolecular proton-transfer dynamics associated with the ketoenolic tautomerization reaction in 2-(2′-hydroxyphenyl)-oxazole is simulated according to a numerically exact quantum-dynamics propagation method and a full-dimensional excited-state potential energy surface, based on an *ab initio* reaction surface Hamiltonian. The reported simulations involve the propagation of 35-dimensional wave packets according to the recently developed matching-pursuit/split-operator-Fourier-transform (MP/SOFT) method by Wu and Batista, [J. Chem. Phys. **121**, 1676 (2004)]. The underlying propagation scheme recursively applies the time-evolution operator as defined by the Trotter expansion to second order accuracy in dynamically adaptive coherent-state expansions. Computations of time-dependent survival amplitudes, photoabsorption cross sections, and time-dependent reactant(product) populations are compared to the corresponding calculations based on semiclassical approaches, including the Herman-Kluk semiclassical initial value representation method. The reported results demonstrate the capabilities of the MP/SOFT method as a valuble computational tool to study ultrafast reaction dynamics in polyatomic systems as well as to validate semiclassical simulations of complex (nonintegrable) quantum dynamics in multidimensional model systems. © *2006 American Institute of Physics*. [DOI: 10.1063/1.2202847]

I. INTRODUCTION

Understanding the molecular mechanisms responsible for excited-state intramolecular proton-transfer (ESIPT) reactions in polyatomic systems is a problem of significant experimental[1–9] and theoretical[10–21] interests. ESIPT reactions are common to a variety of biological processes[22–24] and technological developments,[25] including photostabilizers,[26] and UV filter materials.[27] In general, however, developing an understanding of the detailed molecular mechanisms responsible for ESIPT is hindered by the complexity of polyatomic systems and the intrinsic limitations of current theoretical and experimental methods. Advancing the development of methodologies for understanding ESIPT reactions is thus a central problem of both academic and technological relevances. In particular, ESIPT processes are ideally suited for detailed investigations using newly developed methods for simulations of quantum reaction dynamics. This paper reports the first application of the recently developed matching-pursuit/split-operator-Fourier-transform (MP/SOFT) method[28–32] to studies of the ESIPT dynamics in 2-(2′-hydroxyphenyl)-oxazole (HPO), due to the ultrafast keto-enolic tautomerization reaction depicted in Fig. 1.

ESIPT reactions have been investigated in several experimental studies that focused on molecular systems similar to the HPO molecule,[6,33–39] including the closely related 2-(2′-hydroxyphenyl)-4-methyloxazole (HPMO) molecule.[13,19,21,40] In general, these studies have analyzed dual bands in the fluorescence spectra, where large Stokes shifts indicated the presence of both tautomeric forms (i.e., keto and enolic). In particular, femtosecond fluorescence transient signals of HPMO have been investigated in a variety of aprotic solvents[41] and molecular environments.[40] The assignment of the fluorescent transient signal to the time-dependent reactant (enol) population decay has indicated proton-transfer timescales in the 100–200 fs range with no significant dependence on the molecular environment.[40]

Theoretical studies of ESIPT in polyatomic systems are particularly challenging. The description of excited-state relaxation processes often involves quantum mechanical behavior such as tunneling and interference phenomena. Moreover, the proton quantum motion is usually coupled to the relaxation of the remaining degrees of freedom in the system. Therefore, rigorous treatments find it necessary to integrate explicitly the equations of motion associated with the underlying excited-state quantum reaction dynamics[15,16,21,42] on excited-state potential energy surfaces (PESs) obtained according to *ab initio* quantum chemistry calculations.[13,15,16,19,43]

In recent years, there has been significant progress in the development and application of computational methods for modeling quantum processes,[28–32,44–68] including numerically exact methods for wave-packet propagation[69–81] based on the SOFT method,[82–84] the Chebyshev expansion,[85] or short iterative Lanczos methods.[86] However, establishing rigorous yet practical approaches for simulations of quantum dynamics in systems with many degrees of freedom is still one of the important challenges of modern computational chemistry. In fact, studies of ESIPT reactions have been limited to either applying rigorous propagation methods to

[a]Present address: Department of Chemistry, Tulane University, New Orleans, Louisiana 70118.
[b]Author to whom correspondence should be addressed. Electronic mail: victor.batista@yale.edu

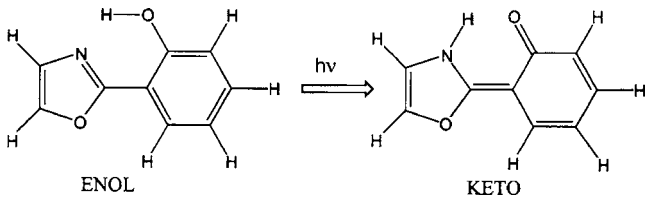

FIG. 1. Molecular structural diagram describing the ultrafast ESIPT due to keto-enolic tautomerization in 2-(2′-hydroxyphenyl)-oxazole (HPO).

reduced-dimensional model systems,[15,16,42,87,88] or conducting simulations on full-dimensional potentials with approximate propagation schemes.[15,16,21,89]

The MP/SOFT method has been recently introduced as a simple and rigorous time-dependent scheme for simulations of quantum processes in multidimensional systems.[28–32] The method is based on the recursive application of the time-evolution operator, as defined by the Trotter expansion to second-order accuracy, in nonorthogonal and dynamically adaptive coherent-state representations generated according to the matching-pursuit algorithm.[90] Such representations allow for an *analytic* implementation of the Trotter expansion, bypassing the exponential scaling problem associated with the usual fast-Fourier transform in the standard grid-based SOFT approach. The main advantage relative to other time-dependent methods based on coherent-state expansions[48,91–100] is that the MP/SOFT approach avoids the usual need of solving a coupled system of differential equations for propagating expansion coefficients. In addition, the matching-pursuit successive orthogonal decomposition scheme (intrinsic to the MP/SOFT method) overcomes the drawback of overcompleteness introduced by nonorthogonal basis functions.[73] Applications of the MP/SOFT method have already included simulations of tunneling dynamics in model systems with up to 20 coupled degrees of freedom[28] and benchmark simulations of nonadiabatic dynamics.[29] In addition, the approach has been generalized to calculations of thermal-equilibrium density matrices, finite-temperature time-dependent expectation values and time-correlation functions.[30]

This paper investigates the capabilities of the MP/SOFT method as applied, for the first time, to simulations of a realistic ESIPT reaction due to photoinduced keto-enolic tautomerization. The reported simulations involve the propagation of 35-dimensional wave packets and the subsequent computation of time-dependent survival amplitudes, photoabsorption cross-sections and time-dependent reactant(product) populations. It is shown that the MP/SOFT approach provides a rigorous description of observables, associated with such a high-dimensional model system, consistent with approximate simulations based on semiclassical and mixed quantum-classical approaches, including the Herman-Kluk semiclassical initial value representation (HK SC-IVR),[15,101] the time-dependent self-consistent field (TDSCF),[102] and the classical Wigner approach.[103] These results allow us to estimate the validity of mechanistic descriptions and quantify the reliability of calculations based on popular semiclassical and mixed quantum-classical methods, where the resulting consequences of the underlying approximations are often difficult to estimate in applications to high-dimensional model systems.

The paper is organized as follows. Section II describes the implementation of the MP/SOFT method in complex-valued coherent-state representations and the computations of time-dependent survival amplitudes, photoabsorption cross sections, and time-dependent reactant(product) populations. Section III describes the computational results obtained according to the MP/SOFT method and the comparison to those obtained with approximate semiclassical methodologies. Section IV summarizes and concludes.

II. METHODS

A. Excited-state potential energy surface

The excited-state intramolecular proton-transfer reaction in HPO is described in terms of the full-dimensional S_1 excited-state PES $V(r_1,r_2,\mathbf{z})$ described in Ref. 15. The PES is constructed as a quadratic expansion around the two-dimensional reaction surface potential $V_0(r_1,r_2)$,

$$V(r_1,r_2,\mathbf{z}) = V_0(r_1,r_2) + \tfrac{1}{2}[\mathbf{z}-\mathbf{z}_0(r_1,r_2)]\mathbf{F}(r_1,r_2)\cdot[\mathbf{z} - \mathbf{z}_0(r_1,r_2)], \quad (1)$$

where r_1 is the proton displacement and r_2 is the lowest frequency in-plane bending mode (170 cm^{-1}), i.e., an internal bending mode that modulates the intramolecular proton donor-acceptor distance. The other 49 vibrational modes in the system are modeled as locally harmonic degrees of freedom $\mathbf{z}$, with *ab initio* force constants $\mathbf{F}(r_1,r_2)$ and equilibrium positions $\mathbf{z}_0(r_1,r_2)$ parametrized by the reaction coordinates r_1 and r_2.

The *ab initio* excited-state reaction surface potential $V_0(r_1,r_2)$ is constructed by fully optimizing the geometry of the system with respect to all other degrees of freedom $\mathbf{z}$, subject to the constraint of fixed r_2 at the geometries of the enol, transition state, and keto tautomeric forms. The values of $\mathbf{z}_0(r_1,r_2)$ at the optimized configurations are obtained by projecting the geometrical difference, with respect to the reference ground-state minimum energy configuration, onto the corresponding normal mode eigenvectors. It is found that the equilibrium positions $\mathbf{z}_0(r_1,r_2)$ associated with the 16 out-of-plane vibrational modes are approximately independent of the reaction coordinates r_1 and r_2. Therefore, the *ab initio* model potential implemented in our calculations includes only the 34 in-plane vibrational modes significantly coupled to the proton displacement, including 33 locally harmonic modes $\mathbf{z}$ and the reaction coordinate r_2.

B. MP/SOFT approach

This section briefly outlines the MP/SOFT methodology, as implemented in simulations of the ESIPT dynamics associated with the keto-enolic tautomerization reaction in HPO. A more thorough description of the MP/SOFT method can be found in previous work.[28]

Consider the propagation of the N-dimensional wave function $\langle \mathbf{x}|\Psi_t\rangle$ by recursively applying the short-time approximation to the time-evolution operator defined by the Trotter expansion to second-order accuracy,

$$e^{-i\hat{H}\tau} \approx e^{-iV(\hat{\mathbf{x}})\tau/2} e^{-i\hat{\mathbf{p}}^2/(2m)\tau} e^{-iV(\hat{\mathbf{x}})\tau/2}. \tag{2}$$

Here, τ is a short propagation time period for the evolution of the system as described by the Hamiltonian $\hat{H}=\hat{\mathbf{p}}^2/(2m)+V(\hat{\mathbf{x}})$. To keep the notation as simple as possible, all expressions are written in mass-weighted coordinates and atomic units, so that all degrees of freedom have the same mass m and $\hbar=1$.

The MP/SOFT implementation of Eq. (2) can be described by the following steps:

- Step 1: Decompose $\langle \mathbf{x}|\tilde{\Psi}_t\rangle \equiv \langle \mathbf{x}|e^{-iV(\hat{\mathbf{x}})\tau/2}|\Psi_t\rangle$ in a matching-pursuit coherent-state expansion (*vide infra*)

$$\langle \mathbf{x}|\tilde{\Psi}_t\rangle \approx \sum_{j=1}^{n} c_j \langle \mathbf{x}|j\rangle, \tag{3}$$

  where $\langle \mathbf{x}|j\rangle$ are N-dimensional coherent states.

- Step 2: Analytically Fourier transform each term in the coherent-state expansion to the momentum representation, apply the kinetic energy part of the Trotter expansion and analytically inverse Fourier transform the resulting expression back to the coordinate representation to obtain the time-evolved wave function:

$$\langle \mathbf{x}|\Psi_{t+\tau}\rangle = e^{-iV(\mathbf{x})\tau/2} \sum_{j=1}^{n} c_j \langle \mathbf{x}|\tilde{j}\rangle. \tag{4}$$

Note that according to this approach, the computational task necessary for quantum propagation is completely reduced to the problem of recursively generating the matching-pursuit coherent-state expansions introduced by Eq. (3).

The basis functions $\langle \mathbf{x}|j\rangle$, introduced by Eq. (3), are N-dimensional coherent states,

$$\langle \mathbf{x}|j\rangle \equiv \prod_{k=1}^{N} A_j(k) e^{-\gamma_j(k)(x(k)-x_j(k))^2/2+ip_j(k)(x(k)-x_j(k))}, \tag{5}$$

with *complex-valued* coordinates $x_j(k)\equiv r_j(k)+id_j(k)$, momenta $p_j(k)\equiv g_j(k)+if_j(k)$, and scaling parameters $\gamma_j(k)\equiv a_j(k)+ib_j(k)$. The normalization constants are $A_j(k) \equiv (a_j(k)/\pi)^{1/4}\exp[-\frac{1}{2}a_j(k)d_j(k)^2 - d_j(k)g_j(k) - (b_j(k)d_j(k)+f_j(k))^2/(2a_j(k))]$. The expansion coefficients c_j, introduced by Eq. (3), are defined as follows: $c_1\equiv\langle 1|\tilde{\Psi}_t\rangle$ and $c_j \equiv \langle j|\tilde{\Psi}_t\rangle - \Sigma_{k=1}^{j-1} c_k\langle j|k\rangle$, for j=2-N. Note that the use of complex-valued x_j and p_j does not require analytic continuation of the potential energy surfaces.

The basis functions $\langle \mathbf{x}|\tilde{j}\rangle$, introduced by Eq. (4), are also N-dimensional coherent states but with arguments defined as follows:

$$\langle \mathbf{x}|\tilde{j}\rangle \equiv \prod_{k=1}^{N} A_j(k) \sqrt{\frac{m}{m+i\tau\gamma_j(k)}} \times \exp\left(\frac{(p_j(k)/\gamma_j(k) - i(x_j(k)-x(k)))^2}{(2/\gamma_j(k)+i2\tau/m)} - \frac{p_j(k)^2}{2\gamma_j(k)}\right). \tag{6}$$

The complex-valued coherent-state expansions, introduced by Eq. (3), are obtained by combining the matching pursuit algorithm and a gradient-based optimization method as follows:

- Step 1.1. Starting from an initial trial coherent state, $|j\rangle$, evolve the real and imaginary components of its complex parameters $x_j(k), p_j(k)$ and $\gamma_j(k)$ and locally maximize the norm of its overlap with the target state, $|\langle j|\tilde{\Psi}_t\rangle|$. The parameters $x_1(k)$, $p_1(k)$, and $\gamma_1(k)$ of the local maximum define the first coherent-state $|1\rangle$ in the expansion and its corresponding expansion coefficient $c_1\equiv\langle 1|\tilde{\Psi}_t\rangle$ as follows: $|\tilde{\Psi}_t\rangle = c_1|1\rangle + |\varepsilon_1\rangle$. Note that the residual vector $|\varepsilon_1\rangle$ is orthogonal to $|1\rangle$ by virtue of the definition of c_1.

- Step 1.2. Go to 1.1, replacing $|\tilde{\Psi}_t\rangle$ by $|\varepsilon_1\rangle$, i.e., subdecompose $|\varepsilon_1\rangle$ by its projection along the direction of its locally optimum match $|2\rangle$ as follows: $|\varepsilon_1\rangle = c_2|2\rangle + |\varepsilon_2\rangle$, where $c_2\equiv\langle 2|\varepsilon_1\rangle$. Note that since $|\varepsilon_2\rangle$ is orthogonal to $|2\rangle$, $|\varepsilon_2| \leqslant |\varepsilon_1|$.

Step 1.2. is repeated each time on the following residue. After n successive projections, the norm of the residual vector $|\varepsilon_n\rangle$ is smaller than a desired precision ϵ—i.e., $|\varepsilon_n| = (1-\Sigma_{j=1}^{n}|c_j|^2)^{1/2} < \epsilon$, and the resulting expansion is given by Eq. (3). Note that although the coherent states are nonorthogonal basis functions, norm conservation is maintained within a desired precision just as in a linear orthogonal decomposition.

It is important to mention that the computational bottleneck of the MP/SOFT method involves the calculation of overlap matrix elements $\langle j|e^{-i\hat{V}(\mathbf{x})\tau/2}|\tilde{k}\rangle$ and $\langle j|e^{-i\hat{V}(\mathbf{x})\tau/2}|k\rangle$. Evaluating these matrix elements involves the computation of 35-dimensional integrals, a task that is trivially parallelized according to a portable single-program-multiple-data (SPMD) streams code that runs under the message-passing-interface (MPI) environment, exploiting the functional form of the excited-state PES introduced by Eq. (1). Partial integration with respect to the 33 harmonic modes z is performed analytically, while integration with respect to the reaction coordinates r_1 and r_2 is efficiently performed according to numerical quadrature techniques.

III. RESULTS

The simulation results obtained according to the MP/SOFT methodology (described in Sec. II B), in conjunction with the full-dimensional S_1 PES (described in Sec. II A), are presented in two sections. First, Sec. III A discusses the photoabsorption spectrum $\sigma(\lambda)$ and the survival amplitudes $\xi(t)$, including comparisons to the corresponding results obtained

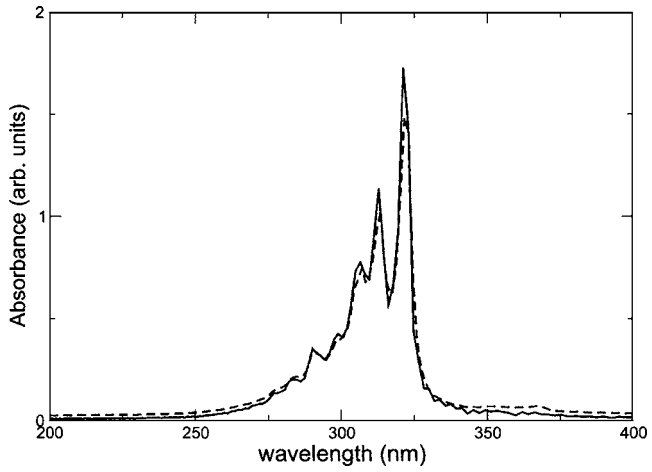

FIG. 2. Comparison of the photoabsorption spectra of HPO obtained according to the MP/SOFT (solid line) and SC-IVR (dashed line) methods, including a phenomenological dephasing time $T_2=35$ fs.

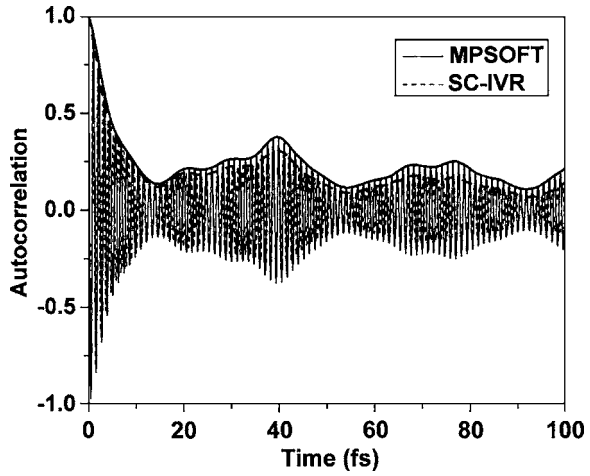

FIG. 3. Comparison of the real-part and modulus of the time-dependent survival amplitude $\xi(t)=\langle\psi_0|\psi_t\rangle$ obtained according to the MP/SOFT (solid line) and SC-IVR (dashed line) methods.

according to approximate methodologies (i.e., the HK SC-IVR,[15,101] the TDSCF method,[102] and the classical Wigner approach[103]). Subsequently, Sec. II B illustrates the capabilities of the MP/SOFT methodology as applied to the description of the time-dependent reactant(enol) population $P(t)$ and the intrinsic decoherence (and partial recoherence) phenomena experienced by the transferring proton due to the interactions with the bath of vibrational modes in HPO.

A. Photoabsorption

Figure 2 shows the comparison of the photoabsorption spectra $\sigma(\lambda)$ of HPO, obtained according to the MP/SOFT and HK SC-IVR methodologies. It is shown that the two methodologies predict essentially the same spectroscopic features, including the spectral position, the overall width and the superimposed vibrational structure (with peaks spaced by ~11 nm). These results indicate that the MP/SOFT method is able to validate HK SC-IVR calculations, providing an interpretation of the photoabsorption spectrum based on the ultrafast ESIPT modulated by vibronic modes.[15] Therefore, such a picture is robust and reproducible by rigorous MP/SOFT calculations where all 35 degrees of freedom in the model system are treated fully quantum mechanically. The extent to which these results are significant is associated with the interpretation of experimental studies of HPMO where the superimposed structure of the photoabsorption spectrum (i.e., peaks at 309 and 322 nm) was assigned to the vertical excitation and the 0-0 transition, respectively.

The photoabsorption spectra $\sigma(\lambda)$, shown in Fig. 2, are computed as the Fourier transform of the survival amplitudes $\xi(t)$,

$$\sigma(\lambda)=\frac{1}{2\pi\hbar}\int_{-\infty}^{\infty}dt\xi(t)e^{i\omega t}, \tag{7}$$

where $\omega=2\pi c/\lambda$, and $\xi(t)\equiv\langle\Psi_0|e^{-i\hat{H}t/\hbar}|\Psi_0\rangle=\langle\Psi_0|\Psi_t\rangle$. Here, $|\Psi_t\rangle$ is the multidimensional time-dependent wave packet evolving on the S_1 PES, described in Sec. II A, and

$$\langle\mathbf{q}|\Psi_0\rangle=\prod_{j=1}^{N}\left(\frac{\alpha_j}{\pi}\right)^{1/4}\exp\left(-\frac{\alpha_j}{2}q(j)^2\right), \tag{8}$$

is the initial state (prepared in the ground electronic state S_0) multiplied by a constant transition-dipole moment (Condon approximation). The parameters introduced by Eq. (8) correspond to $N=35$, the total number of degrees of freedom in the system; $q(j)$ is the jth coordinate; $\alpha_j=\sqrt{k_j\mu^{(j)}/\hbar^2}$, where k_j is the jth harmonic constant; and $\mu^{(j)}$ is the jth reduced mass. In addition to the gas-phase spectra, we compute the corresponding spectra in solution by including a phenomenological dephasing time $T_2=35$ fs, selected to reproduce the line-broadening observed in the experimental HPO absorption spectrum in n-hexane room-temperature solutions.[13] In the time-dependent formalism, the dephasing is achieved simply by multiplying the survival amplitudes $\xi(t)$ by the damping factor e^{-t/T_2} before computing the Fourier-transform introduced by Eq. (7).

Figure 3 shows the comparison of the real part and modulus of the survival amplitude $\xi(t)$, obtained according to the MP/SOFT and SC-IVR methodologies. It is shown that the MP/SOFT computations are in good agreement with the HK SC-IVR results. Both calculation methods result in an initial falloff, within 20 fs, corresponding to the ultrafast relaxation of the system moving away from the Franck-Condon region. The recurrences at later times also coincide for both methods and are due to the wave-packet components associated with higher frequency modes returning back to the initial Franck-Condon configurations. The observed discrepancies in amplitudes are likely due to the lack of norm conservation associated with the time-dependent wave packet as described by the HK SC-IVR propagation scheme.

B. Reactant population decay and decoherence

Figure 4 shows the evolution of the time-dependent reactant(enol) population $P(t)$ due to ESIPT in HPO as described by the MP/SOFT method (solid line), treating all 35 coupled degrees of freedom fully quantum mechanically. Figure 4 also presents the comparison to the corresponding

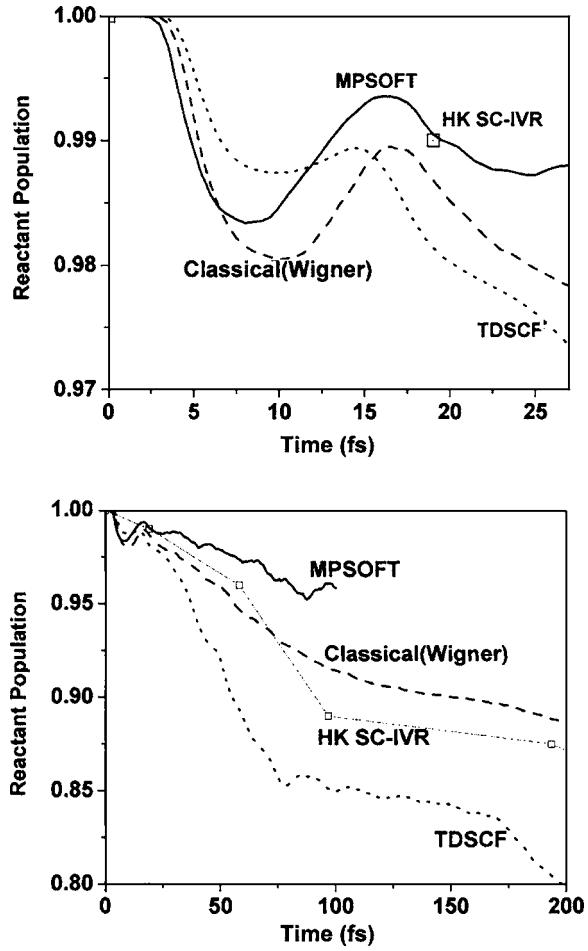

FIG. 4. Time-dependent reactant (enol) population obtained by simulating the ultrafast tautomerization dynamics according to the MP/SOFT method (solid line), the Herman-Kluk SC-IVR (boxes) (Ref. 15), the classical Wigner approach (dashes) and the TDSCF method (short dashes), as described in the text.

results obtained according to more approximate methodologies, including the TDSCF method (dots),[102] the forward-backward HK SC-IVR method (squares),[15] and the classical Wigner approach (dashes).[103]

The employed TDSCF method implements a single-configuration Hartree ansatz,

$$\Psi_t(\mathbf{R},\mathbf{x}) = e^{i\eta(t)}\chi_t(\mathbf{R})\phi_t(\mathbf{x}), \tag{9}$$

where $\eta(t)$ is an overall phase factor and the multidimensional coordinate $\mathbf{R}$ represents five large amplitude coordinates, including the OH stretching mode r_1, the lowest frequency in-plane hydroxyphenyloxazole bending mode r_2 and three other in-plane vibrational modes that are significantly coupled to the reaction coordinates r_1 and r_2. The remaining 30 vibrational modes are represented by the multidimensional coordinate $\mathbf{x}$.

Substituting the ansatz introduced by Eq. (9) into the time-dependent Schrödinger equation, we obtain the well-known self-consistent field equations,[102,104]

$$i\hbar\dot{\phi}_t(\mathbf{x}) = \langle\chi_t|\hat{H}|\chi_t\rangle\phi_t(\mathbf{x}), \tag{10}$$

and

$$i\hbar\dot{\chi}_t(\mathbf{R}) = \langle\phi_t|\hat{H}|\phi_t\rangle\chi_t(\mathbf{R}), \tag{11}$$

where $\phi_t(\mathbf{x})$ is approximated by the Gaussian wave-packet,

$$\phi_t(\mathbf{x}) = \prod_{j=6}^{35}\pi^{-1/4}\exp\left(-\tfrac{1}{2}(x_j-\bar{x}_j(t))^2 + \frac{i}{\hbar}(\bar{p}_j(t)(x_j-\bar{x}_j(t)) + S(t))\right). \tag{12}$$

Here, $\{\bar{x}_j(t),\bar{p}_j(t)\}$ are classical coordinates and momenta evolving according to the effective potential energy surface $V_e(\mathbf{x};t)=\langle\chi_t|\hat{H}|\chi_t\rangle$. These trajectories, as well as the classical action $S(t)$, are computed by numerically integrating Hamilton's equations according to the Velocity-Verlet algorithm.[105] Initial conditions are chosen by importance sampling Monte Carlo, with sampling functions defined by the initial Husimi distribution. Finally, χ_t is propagated according to the MP/SOFT methodology, described in Sec. II B, thereby integrating Eq. (11) self-consistently with Eq. (10).

In contrast to the TDSCF approach, the HK SC-IVR considers all degrees of freedom on equal *semiclassical* dynamical footing. Such SC-IVR method is implemented according to the following "direct" and "correct" forward-backward computational scheme,[15]

$$P(t) = (2\pi\hbar)^{-2N}\int d\mathbf{p}_0\int d\mathbf{q}_0\int d\mathbf{p}_0'\int d\mathbf{q}_0' e^{i(S_t(\mathbf{p}_0,\mathbf{q}_0)-S_t(\mathbf{p}_0',\mathbf{q}_0'))/\hbar}C_t(\mathbf{p}_0,\mathbf{q}_0)\times C_t^*(\mathbf{p}_0',\mathbf{q}_0')\langle\Psi_0|\mathbf{p}_0',\mathbf{q}_0'\rangle\langle\mathbf{p}_t',\mathbf{q}_t'|h|\mathbf{p}_t,\mathbf{q}_t\rangle\langle\mathbf{p}_0,\mathbf{q}_0|\Psi_0\rangle. \tag{13}$$

According to this approach, observables are *directly* computed (i.e., avoiding the need of obtaining first intermediate quantities, such as the time-evolved wave packet) and the dual phase-space integration is explicitly evaluated (i.e., without applying the usual stationary-phase approximation[106,107]). Here, S_t is the classical action and C_t are the Herman-Kluk preexponential factors obtained by propagating the monodromy matrix elements. The operator h, introduced by Eq. (13), is a step function of the transferring proton coordinate r_1, with value 1(0) on the reactant-(product) side of the dividing transition-state surface.

The partial contribution of a single trajectory to $P(t)$ requires forward propagation from the initial phase point $(\mathbf{q}_0,\mathbf{p}_0)$ to the resulting phase point $(\mathbf{q}_t,\mathbf{p}_t)$ at time t. At this

time, the trajectory undergoes a coordinate and momentum stochastic hop $(\mathbf{q}_t,\mathbf{p}_t)\rightarrow(\mathbf{q}_t',\mathbf{p}_t')$ and then evolves backward from $(\mathbf{q}_t',\mathbf{p}_t')$ to the resulting phase point $(\mathbf{q}_0',\mathbf{p}_0')$ at time 0. Therefore, the approach avoids the need of computing first the time-evolved wave packet as an expansion of n coherent-states that would lead to $O(n^2)$ calculations of $P(t)$. The dual phase-space integration in Eq. (13) is performed by importance sampling Monte Carlo where initial conditions $(\mathbf{q}_0,\mathbf{p}_0)$ are sampled according to the coherent-state transform of the initial state $|\Psi_0\rangle$. The coordinates and momenta $(\mathbf{q}_t',\mathbf{p}_t')$ are sampled according to the following sampling function, defined by the overlap of coherent-states,[15]

$$f_t(\mathbf{q}_t',\mathbf{p}_t') = (1-\beta)\prod_{j=1}^{N}(\delta/\pi)^{1/2}e^{-\delta[(p_t'(j)-p_t(j))^2+(q_t'(j)-q_t(j))^2]} + \beta\prod_{j=1}^{N}|\langle p_t'(j),q_t'(j)|p_t(j),q_t(j)\rangle|, \tag{14}$$

where δ is a constant parameter and the convergence rate β is adjusted according to the dimensionality of the problem. The first term, in Eq. (14), provides a localized distribution function for sampling coordinates and momenta $(\mathbf{q}_t',\mathbf{p}_t')$ sufficiently close to $(\mathbf{q}_t,\mathbf{p}_t)$, ensuring partial cancellation of the phase in the integrand. The second term provides an upper bound to the variance when the first term is much smaller than the value of the integrand.

Finally, the Wigner approach considers all degrees of freedom to be *classical* dynamical variables, evolving according to Hamilton's equations of motion from initial conditions sampled according to the Wigner distribution function.[15,103] The resulting time-dependent reactant (enol) probability is estimated as

$$P(t) = (2\pi\hbar)^{-2N}\int d\mathbf{q}_0\int d\mathbf{p}_0 F^W(\mathbf{q}_0,\mathbf{p}_0)h(\mathbf{q}_t), \tag{15}$$

where

$$F^W(\mathbf{q}_0,\mathbf{p}_0) = \int_{-\infty}^{\infty} d\Delta\mathbf{q}\, e^{i\mathbf{p}_0\Delta\mathbf{q}/\hbar}\Psi_0^*(\mathbf{q}_0-\Delta\mathbf{q}/2)\Psi_0(\mathbf{q}_0+\Delta\mathbf{q}/2). \tag{16}$$

Therefore, the classical Wigner computation of $P(t)$ does not include interference effects since, according to Eq. (15), $P(t)$ is determined simply by the number of members of the ensemble found with reactant configurations at time t.

Figure 4 shows that, according to the MP/SOFT calculations, less than 5% of the initial enol population is expected to be isomerized within 100 fs after photoexcitation of the system (i.e., a slightly slower initial relaxation than predicted by the semiclassical methodologies). It is important to note, however, that the descriptions provided by the HK SC-IVR and the Wigner classical methodologies are remarkably accurate within the early 25 fs of dynamics. These results indicate that the initial (Husimi and Wigner) distributions properly describe the initial proton tunneling event as determined by the zero-point energy motion. At longer times, however, interference and recrossing events make semiclassical results less reliable.

The results shown in Fig. 4 suggest that (at least for this particular ESIPT problem) the classical Wigner approach and the HK SC-IVR methodology provide results of similar accuracy. These approximate results are in more favorable agreement with MP/SOFT calculations than those obtained according to the TDSCF methodology, which is surprising since the classical Wigner approach should be less reliable than the TDSCF method (where some coordinates are treated quantum mechanically and only the remaining evolve classically in a mean-field potential). In practice, however, it is found that considering the evolution of different degrees of freedom on different dynamical footing introduces inaccuracies that are more significant than the accounted quantum corrections.

For completeness, in order to demonstrate convergence of the MP/SOFT results at the level of wave functions, Fig. 5 shows the time evolution of the 35-dimensional wave packet reduced to the space of reaction coordinates r_1 and r_2. These results are converged with respect to the MP/SOFT procedure and show good qualitative agreement with the description of dynamics provided by benchmark calculations of ESIPT in a simplified three-dimensional model system reported in Ref. 15.

In order to analyze the extent of intrinsic decoherence associated with proton-motion during the course of the keto-enolic tautomerization, we consider $\rho(t)$, which is the reduced density matrix associated with the proton coordinate (i.e., the density matrix obtained by tracing out all of the degrees of freedom except for the proton coordinate) and we compute the time-dependent quantity $\mathrm{Tr}[\rho^2(t)]$. Initially, $\mathrm{Tr}[\rho^2(0)]=1$ since the OH stretching mode is prepared in a pure state (i.e., the ground state). However, as the reaction proceeds and the proton-motion becomes coupled to the remaining degrees of freedom, the state of the proton becomes mixed and $\mathrm{Tr}[\rho^2(t)]<1$. The quantity $\mathrm{Tr}[\rho^2(t)]$ thus serves as a standard measure of decoherence.[89,104,108,109]

Figure 6 shows that $\mathrm{Tr}[\rho^2(t)]$ exhibits an initial decoherence falloff within 4 fs and then oscillates with a period of about 8 fs, mostly determined by the OH vibrational period. The semiquantitative agreement with the HK SC-IVR results at early times indicates that the HK semiclassical methodology is able to properly describe the 4 fs decoherence time as well as the recoherence phenomena observed at 8 fs. The deviations observed at longer times, however, illustrate typical convergence difficulties faced by the HK SC-IVR when applied to the description of decoherence in this 35-dimensional model system.

The MP/SOFT expansions of the HPO time-dependent wave packet are rather compact and usually converge with $n\sim10^2$ coherent states, probably due to the intrinsic simplicity of the couplings in the reaction surface Hamiltonian where vibrational modes are only indirectly coupled through the reaction coordinates. Nonetheless, calculations are still computationally intensive since the MP/SOFT coherent-state expansions need to be regenerated for each propagation step. While computationally demanding, MP/SOFT calculations can be trivially parallelized and become less costly than computations based on the HK SC-IVR, which usually require the propagation of $n\sim10^6-10^7$ classical trajectories,

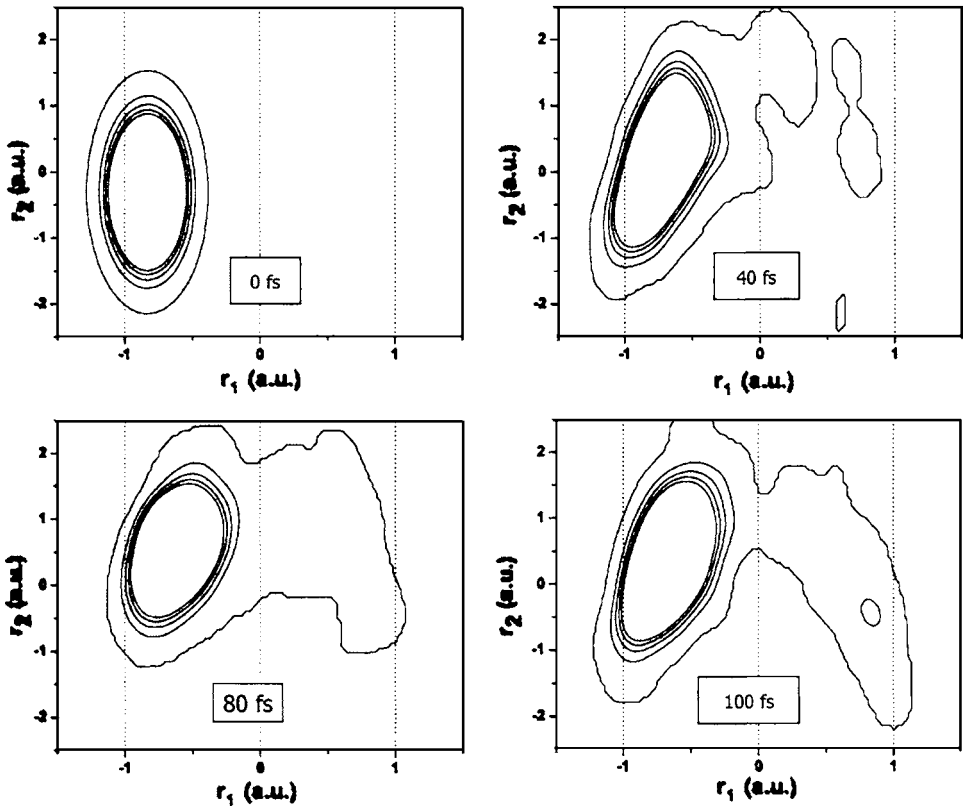

FIG. 5. Comparison of the time-dependent wave packet $\rho_t(r_1,r_2) = \int d\mathbf{z}|\Psi_t^*(r_1,r_2,\mathbf{z})|^2$, reduced to the space of reaction coordinates r_1 and r_2, at various different times during the early time relaxation after photoexcitation of the system. Wave packets are represented by five contour lines equally spaced by 0.045 units in the 0.005–0.185 range of amplitude in order to allow for comparisons with a simplified 3-dimensional model discussed in Fig. 9 of Ref. 15.

making HK SC-IVR computations of $P(t)$ or $\mathrm{Tr}[\rho^2(t)]$ feasible only when performed according to the "direct" approach implemented in our study. Otherwise, the evaluation of these quantities would be computationally intractable $O(n^2)$ calculations.

IV. CONCLUDING REMARKS

In this paper we have shown how the ESIPT associated with the keto-enolic tautomerization reaction of HPO can be investigated according to full quantum mechanical methods, without the need of invoking any kind of classical or semiclassical approximation, or reduced dimensionality models.

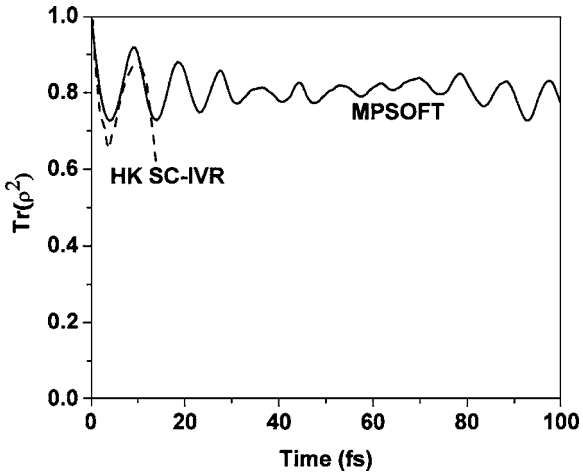

FIG. 6. Comparison of the time-dependent $\mathrm{Tr}[\rho^2(t)]$, during the first 100 fs of dynamics, obtained according to the MP/SOFT (solid line) and the Herman-Kluk SC-IVR (dashes)[15] methods.

The study involves the propagation of 35-dimensional wave packets, applying the MP/SOFT methodology in conjunction with a model Hamiltonian based on an *ab initio* S_1 PES. The MP/SOFT propagation scheme recursively applies the time-evolution operator, as defined by the Trotter expansion to second order accuracy, in dynamically adaptive coherent-state expansions. Such representations are particularly suitable for applications to high-dimensional problems since they allow for an *analytic* implementation of the Trotter expansion, bypassing the exponential scaling problem associated with the usual fast-Fourier transform in the standard grid-based SOFT approach. The reported calculations constitute the first application of this novel time-dependent MP/SOFT methodology to a realistic ESIPT reaction in a polyatomic model system.

We have demonstrated the capabilities of the MP/SOFT approach as applied to the description of the HPO photoabsorption spectrum and the time-dependent reactant population. The MP/SOFT method also successfully describes the underlying decoherence and recoherence phenomena due to coupling interactions between the proton-motion and the relaxation of the remaining degrees of freedom in the system. It is therefore concluded that the reported MP/SOFT calculations at least demonstrate the potentiality of a rigorous, yet practical, quantum-dynamics methodology for studying excited-state intramolecular proton transfer dynamics, coupled to the relaxation of many other degrees of freedom in a realistic model of a polyatomic system. Furthermore, we have shown that the MP/SOFT approach allows an evaluation of the validity (i.e., the error range) of calculations based on popular mixed quantum-classical and semiclassical approaches, including HK SC-IVR, the TDSCF method and the

classical Wigner approach, as applied to the description of complex quantum dynamics. It is concluded that treatments that rely upon a description of all degrees of freedom on equal dynamical footing are expected to provide more accurate results than mixed quantum-classical approaches based on mean-field approximations. In particular, comparisons with MP/SOFT results demonstrates that the HK SC-IVR provides an overall description of dynamics in semiquantitative agreement with full quantum calculations of the absorption spectrum, survival amplitudes, reactant populations, and the decoherence measure $\mathrm{Tr}[\rho^2(t)]$.

Finally, we have shown that the dynamical picture emerging from the MP/SOFT study is consistent with the reaction mechanism suggested by the HK SC-IVR,[15] wherein ESIPT is modulated by a low-frequency (177 cm^{-1}) in-plane internal bending mode that affects the intermoiety proton donor-acceptor distance. Showing that the proposed mechanism is robust and reproducible in terms of rigorous quantum dynamics methods is important since experimental studies of HPMO have proposed a different molecular mechanism of ESIPT modulated by out-of-plane twisting motions.[40] Furthermore, we have shown that the MP/SOFT and HK SC-IVR methodologies have semiquantitative agreement with each other in the description of the HPO photoabsorption spectrum. Indeed, both methods predict an asymmetric absorption band in the 300–330 nm range with a diffuse superimposed structure with peaks spaced by ~11 nm. The MP/SOFT method predicts, however, that the early time relaxation dynamics is slightly slower than predicted according to semiclassical methodologies. Further, in qualitative agreement with the HK SC-IVR description, the MP/SOFT calculations predict that the decoherence time and the oscillatory recoherence dynamics are strongly modulated by the OH stretching mode.

Finally, we have shown that the efficiency of the matching-pursuit algorithm allows one to provide an explicit description of complex quantum dynamics of multidimensional wave packets in terms of compact and dynamically adaptive coherent state expansions. A drawback of the MP/SOFT approach, however, is that the expansions must be regenerated for each propagation step. While the underlying computational task is demanding, it can be trivially parallelized and moreover efficiently evaluated for reaction surface Hamiltonians where most of the degrees of freedom are harmonic and indirectly coupled to a few reaction coordinates. Work in progress in our group involves the development of efficient implementation strategies suitable for a more general class of Hamiltonians. These techniques avoid the need of numerically computing multidimensional overlap integrals simply by implementing matching pursuit of the corresponding integrands, instead. The capabilities of these more general implementation methods, however, remains to be demonstrated.

ACKNOWLEDGMENTS

One of the authors (V.S.B.) acknowledges a generous allocation of supercomputer time from the National Energy Research Scientific Computing (NERSC) center and financial support from Research Corporation, Research Innovation Award No. RI0702, a Petroleum Research Fund Award from the American Chemical Society PRF No. 37789-G6, a junior faculty award from the F. Warren Hellman Family, the National Science Foundation (NSF) Career Program Award CHE No. 0345984, the NSF Nanoscale Exploratory Research (NER) Award ECS No. 0404191, the Alfred P. Sloan Fellowship (2005-2006), a Camille Dreyfus Teacher-Scholar Award for 2005, and a Yale Junior Faculty Fellowship in the Natural Sciences (2005-2006). The authors thank Mr. Sabas G. Abuabara for proof-reading the manuscript.

[1] J. L. Herek, S. Pedersen, L. Banares, and A. H. Zewail, J. Chem. Phys. **97**, 9046 (1992).
[2] W. Frey, F. Laermer, and T. Elsaesser, J. Phys. Chem. **95**, 0391 (1991).
[3] S. Lochbrunner, K. Stock, and E. Riedle, J. Mol. Struct. **700**, 13 (2004).
[4] C. Chudoba, E. Riedle, M. Pfeiffer, and T. Elsaesser, Chem. Phys. Lett. **263**, 622 (1996).
[5] T. Fiebig, M. Chachisvilis, M. Manger, A. H. Zewail, A. Douhal, I. Garcia-Ochoa, and A. D. H. Ayuso, J. Phys. Chem. A **103**, 7419 (1999).
[6] S. Ameer-Beg, S. M. Ormson, R. G. Brown, P. Matousek, M. Towrie, E. T. J. Nibbering, P. Foggi, and F. V. R. Neuwahl, J. Phys. Chem. A **105**, 3709 (2001).
[7] A. N. Bader, V. G. Pivovarenko, A. P. Demchenko, F. Ariese, and C. Gooijer, J. Phys. Chem. B **108**, 10589 (2004).
[8] P. Toele and M. Glasbeek, Chem. Phys. Lett. **407**, 487 (2005).
[9] K. Sakota, C. Okabe, N. Nishi, and H. Sekiya, J. Phys. Chem. A **109**, 5245 (2005).
[10] U. Nagashima, S. Nagaoka, and S. Katsumata, J. Phys. Chem. **95**, 8532 (1991).
[11] A. L. Sobolewski and W. Domcke, Chem. Phys. Lett. **211**, 82 (1993).
[12] X. F. Duan and S. Scheiner, Chem. Phys. Lett. **204**, 36 (1993).
[13] V. Guallar, M. Moreno, J. M. Lluch, F. Amat-Guerri, and A. Douhal, J. Phys. Chem. **100**, 9789 (1996).
[14] A. L. Sobolewski and W. Domcke, Chem. Phys. Lett. **300**, 533 (1999).
[15] V. Guallar, V. S. Batista, and W. H. Miller, J. Chem. Phys. **113**, 9510 (2000).
[16] V. Guallar, V. S. Batista, and W. H. Miller, J. Chem. Phys. **110**, 9922 (1999).
[17] S. Scheiner, J. Phys. Chem. A **104**, 5898 (2000).
[18] G. Granucci, J. T. Hynes, P. Millie, and T. H. Tran-Thi, J. Am. Chem. Soc. **122**, 12243 (2000).
[19] R. Casadesus, M. Moreno, and J. M. Lluch, Chem. Phys. Lett. **356**, 423 (2002).
[20] J. R. Roscioli, D. W. Pratt, Z. Smedarchina, W. Siebrand, and A. Fernandez-Ramos, J. Chem. Phys. **120**, 11351 (2004).
[21] O. Vendrell, M. Moreno, J. M. Lluch, and S. Hammes-Schiffer, J. Phys. Chem. B **108**, 6616 (2004).
[22] D. P. Zhong, A. Douhal, and A. H. Zewail, Proc. Natl. Acad. Sci. U.S.A. **97**, 14056 (2000).
[23] M. Chattoraj, B. A. King, G. U. Bublitz, and S. G. Boxer, Proc. Natl. Acad. Sci. U.S.A. **93**, 8362 (1996).
[24] P. Miskovsky, Int. J. Photoenergy **4**, 45 (2002).
[25] R. C. Haddon and F. H. Stillinger, *Molecular Electronic Devices* (Marcel Dekker, New York, 1987).
[26] D. A. Parthenopoulos, D. McMorrow, and M. Kasha, J. Phys. Chem. **95**, 2668 (1991).
[27] S. Moller, K. B. Andersen, J. Spanget-Larsen, and J. Waluk, Chem. Phys. Lett. **291**, 51 (1998).
[28] Y. Wu and V. S. Batista, J. Chem. Phys. **121**, 1676 (2004).
[29] Y. Wu, M. F. Herman, and V. S. Batista, J. Chem. Phys. **122**, 114114 (2005).
[30] X. Chen, Y. Wu, and V. S. Batista, J. Chem. Phys. **122**, 64102 (2005).
[31] Y. Wu and V. S. Batista, J. Chem. Phys. **118**, 6720 (2003).
[32] Y. Wu and V. S. Batista, J. Chem. Phys. **119**, 7606 (2003).
[33] T. Arthenengeland, T. Bultmann, N. P. Ernsting, M. A. Rodriguez, and W. Thiel, Chem. Phys. **163**, 43 (1992).
[34] P. Barbara, P. K. Walsh, and L. E. Brus, J. Phys. Chem. **93**, 29 (1989).
[35] G. Yang, F. Morlet-Savary, Z. Peng, S. Wu, and J. Fouassier, Chem. Phys. Lett. **256**, 536 (1996).

[36] L. Premvardhan and L. Peteanu, Chem. Phys. Lett. **296**, 521 (1998).
[37] A. Douhal, F. Amat-Guerri, A. U. Acuna, and K. Yoshihara, Chem. Phys. Lett. **217**, 619 (1994).
[38] A. Dohual, F. Amat-Guerri, and A. U. Acuna, J. Phys. Chem. **99**, 76 (1995).
[39] A. Douhal, F. Lahmani, A. Zehnacker-Rentien, and F. Amat-Guerri, J. Phys. Chem. **98**, 12198 (1994).
[40] A. Douhal, F. Lahmani, A. Zehnacker-Rontien, and F. Amat-Guerri, *AIP Conference Proceedings* No. 346 (AIP, New York, 1995).
[41] M. Chachisvilis, T. Fiebig, A. Douhal, and A. H. Zewail, J. Phys. Chem. A **102**, 669 (1998).
[42] M. Petkovic and O. Kuhn, J. Phys. Chem. A **107**, 8458 (2003).
[43] R. Casadesus, M. Moreno, and J. M. Lluch, J. Photochem. Photobiol., A **173**, 365 (2005).
[44] N. Makri, Annu. Rev. Phys. Chem. **50**, 167 (1999), and referenced therein.
[45] M. H. Beck, A. Jackle, G. A. Worth, and H. D. Meyer, Phys. Rep., Phys. Lett. **324**, 1 (2000).
[46] W. H. Miller, Proc. Natl. Acad. Sci. U.S.A. **102**, 6660 (2005).
[47] M. Ben-Nun, J. Quenneville, and T. J. Martinez, J. Phys. Chem. A **104**, 5161 (2000).
[48] M. Ben-Nun and T. J. Martinez, Adv. Chem. Phys. **121**, 439 (2002).
[49] S. Y. Kim and S. Hammes-Schiffer, J. Chem. Phys. **119**, 4389 (2003).
[50] H. B. Wang and M. Thoss, J. Phys. Chem. A **107**, 2126 (2003).
[51] P. H. Nguyen and G. Stock, J. Chem. Phys. **119**, 11350 (2003).
[52] D. V. Shalashilin and M. S. Child, Chem. Phys. **304**, 103 (2004).
[53] Q. Shi and E. Geva, J. Chem. Phys. **121**, 3393 (2004).
[54] A. Donoso and C. C. Martens, J. Chem. Phys. **116**, 10598 (2002).
[55] O. V. Prezhdo and Y. V. Pereverzev, J. Chem. Phys. **113**, 6557 (2000).
[56] T. D. Hone and G. A. Voth, J. Chem. Phys. **121**, 6412 (2004).
[57] S. Bonella and D. F. Coker, J. Chem. Phys. **114**, 7778 (2001).
[58] A. E. Cardenas, R. Krems, and R. D. Coalson, J. Phys. Chem. A **103**, 9469 (1999).
[59] L. Turi and P. J. Rossky, J. Chem. Phys. **120**, 3688 (2004).
[60] M. Nest and P. Saalfrank, Chem. Phys. **268**, 65 (2001).
[61] S. J. Jang and J. S. Cao, J. Chem. Phys. **114**, 9959 (2001).
[62] A. Sergi, D. MacKernan, G. Ciccotti, and R. Kapral, Theor. Chem. Acc. **110**, 49 (2003).
[63] D. E. Makarov andH. Metiu, J. Chem. Phys. **111**, 10126 (1999).
[64] S. S. Zhang and E. Pollak, J. Chem. Phys. **119**, 11058 (2003).
[65] D. Antoniou andS. D. Schwartz, J. Chem. Phys. **119**, 11329 (2003).
[66] J. L. Gao and D. G. Truhlar, Annu. Rev. Phys. Chem. **53**, 467 (2002).
[67] M. H. M. Olsson, P. E. M. Siegbahn, and A. Warshel, J. Am. Chem. Soc. **126**, 2820 (2004).
[68] I. R. Craig and D. E. Manolopoulos, J. Chem. Phys. **121**, 3368 (2004).
[69] D. Neuhauser, J. Chem. Phys. **100**, 9272 (1994).
[70] W. Zhu, J. Z. H. Zhang, and D. H. Zhang, Chem. Phys. Lett. **292**, 46 (1998).
[71] G. C. Schatz, M. S. Fitzcharles, and L. B. Harding, Faraday Discuss. **84**, 359 (1987).
[72] D. C. Clary, J. Phys. Chem. **98**, 10678 (1994).
[73] R. Kosloff, Annu. Rev. Phys. Chem. **45**, 145 (1994).
[74] J. R. Fair, D. Schaefer, R. Kosloff, andD. J. Nesbitt, J. Chem. Phys. **116**, 1406 (2002).
[75] J. Echave and D. C. Clary, J. Chem. Phys. **100**, 402 (1994).
[76] H. G. Yu and J. T. Muckerman, J. Chem. Phys. **117**, 11139 (2002).
[77] M. I. Hernandez and D. C. Clary, J. Chem. Phys. **101**, 2779 (1994).
[78] D. Charlo and D. C. Clary, J. Chem. Phys. **117**, 1660 (2002).
[79] J. M. Bowman, J. Phys. Chem. A **102**, 3006 (1998).
[80] D. Q. Xie, R. Q. Chen, and H. A. Guo, J. Chem. Phys. **112**, 5263 (2000).
[81] S. M. Anderson, T. J. Park, and D. Neuhauser, Phys. Chem. Chem. Phys. **1**, 1343 (1999).
[82] M. D. Feit, J. A. Fleck, and A. Steiger, J. Comput. Phys. **47**, 412 (1982).
[83] M. D. Feit and J. A. Fleck, J. Chem. Phys. **78**, 301 (1983).
[84] D. Kosloff and R. Kosloff, J. Comput. Phys. **52**, 35 (1983).
[85] H. Tal-Ezer and R. Kosloff, J. Chem. Phys. **81**, 3967 (1984).
[86] T. J. Park and J. C. Light, J. Chem. Rev. 85, 5870 (1986).
[87] J. D. Coe and T. J. Martinez, J. Am. Chem. Soc. **127**, 4560 (2005).
[88] J. D. Coe and T. J. Martinez, J. Chem. Phys. **110**, 618 (2006).
[89] V. S. Batista and P. Brumer, Phys. Rev. Lett. **89**, 143201 (2002).
[90] S. G. Mallat and Z. F. Zhang, IEEE Trans. Signal Process. **41**, 3397 (1993).
[91] E. J. Heller, Chem. Phys. Lett. **34**, 321 (1975).
[92] M. J. Davis and E. J. Heller, J. Chem. Phys. **71**, 3383 (1979).
[93] E. J. Heller, J. Chem. Phys. **75**, 2923 (1981).
[94] R. D. Coalson and M. Karplus, Chem. Phys. Lett. **90**, 301 (1982).
[95] S. I. Sawada, R. Heather, B. Jackson, and H. Metiu, Chem. Phys. Lett. **83**, 3009 (1985).
[96] K. G. Kay, J. Chem. Phys. **91**, 170 (1989).
[97] D. V. Shalashilin and B. Jackson, Chem. Phys. Lett. **291**, 143 (1998).
[98] L. M. Andersson, J. Chem. Phys. **115**, 1158 (2001).
[99] D. V. Shalashilin and M. S. Child, J. Chem. Phys. **113**, 10028 (2000).
[100] D. V. Shalashilin and M. S. Child, J. Chem. Phys. **115**, 5367 (2001).
[101] M. F. Herman and E. Kluk, Chem. Phys. **91**, 27 (1984).
[102] R. B. Gerber, V. Buch, and M. A. Ratner, J. Chem. Phys. **77**, 3022 (1982).
[103] E. J. Heller, J. Chem. Phys. **65**, 1289 (1976).
[104] S. Flores and V. S. Batista, J. Phys. Chem. B **108**, 6745 (2003).
[105] W. Swope, H. Andersen, P. Berens, and K. Wilson,J. Chem. Phys. **76**, 637 (1982).
[106] V. S. Batista, M. T. Zanni, B. J. Greenblatt, D. M. Neumark, and W. H. Miller, J. Chem. Phys. **110**, 3736 (1999).
[107] N. Makri and K. Thompson, J. Chem. Phys. **110**, 1343 (1999).
[108] E. Joos and H. D. Zeh, Z. Phys. B: Condens. Matter **59**, 223 (1985).
[109] W. H. Zurek, Phys. Rev. D **26**, 1862 (1981).